Ocean Spectra for the High-frequency Waves as Determined from Airborne Radar Measurements[1]

G. R. Valenzuela, M. B. Laing, and J. C. Daley

Naval Research Laboratory
Washington, D.C. 20390

ABSTRACT

The possibilities of using radar to obtain oceanographic information are described. Ocean spectra for the short gravity and gravity-capillary waves have been derived from radar cross-section measurements for vertical polarization at 428 MHz, 1228 MHz, 4455 MHz, and 8910 MHz. The average power law of the ocean spectra for these high wave numbers and for strong winds is -3.721, which is in reasonable agreement with Kinsman's (1961) observations on the behavior of the spectrum in the equilibrium range. A "dip" in the spectrum toward the gravity-capillary region (these water waves absent) for a calm sea has been observed. Cox (1958) observed a similar phenomenon in a wave tank, for the slope spectrum.

The exponential growth of gravity-capillary waves has been obtained for light winds, using the wind dependence of the radar cross-section data; for strong winds the wind dependence of the radar cross section (ocean spectrum) is in agreement with the -3.721 power law of the spectra.

1. *Introduction.* Bragg resonant scattering is one of the most important mechanisms that participates in the scattering of electromagnetic waves from liquid surfaces. Previously, Strutt (Lord Rayleigh 1894), studying the reflection of acoustic waves from corrugated surfaces, observed that a resonant condition determined the directions in which the incident wave was scattered; and Rice (1951), in treating the scattering of electromagnetic waves from random slightly rough surfaces, also found resonant scattering to be the main mechanism that contributes to the scattered power. Using Rice's theory, Peake (1959) obtained the first-order Radar Cross Sections (RCS) from the power backscattered by a dielectric and slightly rough surface; his theoretical results were in agreement with experimental measurements on asphalt and concrete roadways. Valenzuela (1967) investigated the significance of the second-order solutions in Rice's theory and applied them to the sea surface.

1. Accepted for publication and submitted to press 17 November 1970.

The experimental confirmation of the Bragg resonant scattering on the sea and on liquid surfaces was demonstrated by Crombie (1955) and Wright (1966). Other investigations, which also support resonant scattering, are those by Wright (1968), Valenzuela and Laing (1970), Guinard and Daley (1970), and Wright and Keller (in press).

The purpose of this paper is to show that resonant scattering makes radar a convenient instrument for obtaining oceanographic information for high-frequency water waves. In the course of this study, radar measurements taken with the Naval Research Laboratory Four-Frequency Radar (4FR) at 428 MHz (UHF), 1228 MHz (L band), 4455 MHz (C band), and 8910 MHz (X band) off New Jersey in December 1964, off Puerto Rico in July 1965, and in the North Atlantic in February 1969 were used in the analysis. A description of the 4FR System is not given here; see Guinard and Daley (1970) or Guinard et al. (in press).

A review of the resonant scattering theory is necessary for introducing the composite model, which has been very successful in predicting the RCS of the sea, using the equilibrium spectrum of the surface roughness. Since the measured RCS of the sea for vertical polarization is approximately equal to the RCS predicted by a slightly rough scattering theory, oceanographic wave-height spectra then may be simply obtained from the RCS data for vertical polarization without considering the composite nature of the surface. The wind dependence of the RCS of the sea, for vertical polarization, may also be investigated by using different radar frequencies. For light winds, the exponential growth of gravity-capillary water waves is found from the C-band and X-band RCS. The wind dependence of the RCS in the saturation or plateau region (strong winds) will be shown to be in reasonable agreement with the power law obtained for the spectra.

2. *The Composite Surface-scattering Model and Background.* The composite-scattering model used to predict the RCS of the sea was developed by Wright (1966, 1968) and, independently, by Fuks (1966) and Semyonov (1966). The model is based on the slightly rough scattering theories for surfaces that have gentle slopes and a roughness scale that is small compared with the wavelength of the incident electromagnetic radiation. To first order, the amplitude of the scattered field in a given direction is purely a function of the amplitude of a particular frequency of roughness on the surface. For example, for back-scattering, only ripples of wavenumber $K = 2\beta \sin \theta$ contribute to the radar return, where $\beta = 2\pi/\lambda$ is the propagation constant of the incident plane wave, and θ is the angle of incidence with respect to the normal to the mean-flat surface.

Strictly speaking, the sea cannot be considered a slightly rough surface for a given radar frequency. For example, for the range of frequencies in the 4FR System, the Bragg resonant water waves range from gravity waves of about

2-m wavelength (UHF at 80° depression angle) to capillary waves of 1.68-cm wavelength (for the X band near grazing). The net effect of the larger gravity waves is to tilt "patches" of slightly rough scatterers and alter the RCS of the sea for a given depression angle. Thus, the normalized RCS,[2] $\sigma_0(\theta)$, given by the slightly rough scattering theories, must be averaged over the distribution of the slopes of the water waves of larger wavelength than the Bragg resonant scatterers. The averaging is performed directly on the RCS, which is proportional to the backscattered power, because the fields from the various "patches" of the slightly rough surface add incoherently. A "patch" of slightly rough surface in an arbitrary position is expressed in terms of two orthogonal rotations of the unit-normal vector to the mean-flat surface of the "patch"; see Wright (1968). A rotation of the normal in the plane of incidence changes only the net angle of incidence while a rotation perpendicular to the plane of incidence yields a mixing of the local backscattered fields; Valenzuela (1968) has investigated this last rotation in detail.

Here it will not be necessary to include the second-order fields backscattered from the patch; however, these cannot be neglected in studies on depolarization. The first-order normalized RCS for a slightly rough "patch" are:

(i) for horizontal polarization,

$$\left.\begin{aligned}\sigma_0(\theta_i)_{HH} = {} & 4\pi\beta^4 \cot^4\theta_i\,|\alpha^2\cos^2\delta\, T_{\perp\perp} + \sin^2\delta[\varepsilon(1+\alpha_i^2) \\ & -\alpha_i^2]\, T_{\parallel\parallel}|^2 W(2\beta\alpha, 2\beta\gamma\sin\delta),\end{aligned}\right\} \tag{1}$$

(ii) for vertical polarization,

$$\left.\begin{aligned}\sigma_0(\theta_i)_{VV} = {} & 4\pi\beta^4 \cot^4\theta_i\,|\alpha^2\cos^2\delta[\varepsilon(1+\alpha_i^2) - \alpha_i^2]\, T_{\parallel\parallel} \\ & + \sin^2\delta\, T_{\perp\perp}|^2 W(2\beta\alpha, 2\beta\gamma\sin\delta),\end{aligned}\right\} \tag{2}$$

where $\cos\theta_i = \cos(\theta + \Psi)\cos\delta$, $\alpha = \sin(\theta+\Psi)$, Ψ and δ are the tilt angles "in," and perpendicular to, the plane of incidence,

$$T_{\perp\perp} = (\varepsilon - 1)/(\gamma_i + \gamma^{\text{II}})^2, \quad T_{\parallel\parallel} = (\varepsilon - 1)/(\varepsilon\gamma_i + \gamma^{\text{II}})^2, \quad \gamma_i = \cos\theta_i;$$

$\alpha_i = \sin\theta_i$, $\gamma^{\text{II}} = (\varepsilon - \alpha_i^2)^{1/2}$, ε is the complex dielectric constant of the surface, and $W(K_x, K_y)$ is the energy spectral density of the surface roughness (ocean wave-height spectrum), defined as: (mean-square height) $= {}^1/_4 \int_{-\infty}^{\infty} dK_x \int_{-\infty}^{\infty} dK_y\, W(K_x, K_y)$.

For the sea, the average RCS, $\sigma_0(\theta)^{\text{SEA}}$, according to the composite surface scattering model, can be obtained from

$$\sigma_0(\theta)^{\text{SEA}} = \int_{-\infty}^{\infty} d(\tan\Psi) \int_{-\infty}^{\infty} d(\tan\delta)\, \sigma_0(\theta_i)\, p(\tan\Psi, \tan\delta), \tag{3}$$

2. $\sigma_0/4\pi \equiv$ average power scattered per unit of solid angle per unit of area of surface divided by the incident power at unit area of surface.

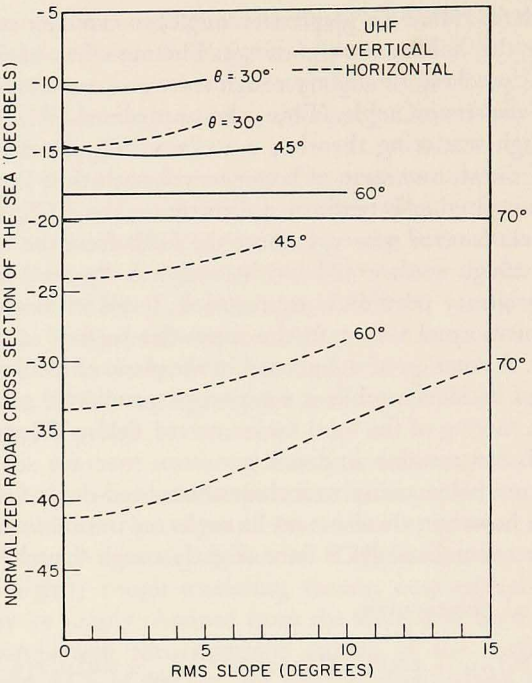

Figure 1. Normalized RCS of the sea, for UHF, from the composite model (first-order fields) versus the RMS slope of the low-frequency water waves, for angle of incidences of 30°, 45°, 60°, and 70°.

where $\sigma_0(\theta_i)$ in the integrand is (1) or (2), depending on the polarization of interest, and $p(\tan \Psi, \tan \delta)$ is the probability density of slopes for water waves that are larger than the Bragg scatterers. Cox and Munk (1954) found the slopes in the sea to be approximately Gaussian, thus

$$p(\tan \Psi, \tan \delta) = (2\pi S_1 S_2)^{-1} \exp\left\{-\frac{\tan^2 \Psi}{2S_1^2} - \frac{\tan^2 \delta}{2S_2^2}\right\}, \tag{4}$$

where S_1^2 and S_2^2 are the variances of slopes in two orthogonal directions on the surface. In general, the directivity of the sea is variable; thus, for general-purpose calculations, we take $S_1^2 = S_2^2 = S^2$, which applies for a nondirectional or confused sea.

The contribution to the variance of slopes from water waves of wavenumbers $K_1 \leq K \leq K_2$ is logarithmic for a spectrum with a Phillips (1958) power law for the equilibrium range [i.e., $W(K) \sim K^{-4}$)]; hence

$$S^2 = 6 \times 10^{-3} \log\left(\frac{K_2}{K_1}\right), \tag{5}$$

where the constant has been taken from Wright (1968).

For a fully developed sea it is possible to take $K_1 = gU^{-2}$ and $K_2 = 2\beta \sin\theta$, the Bragg resonant wavenumber, where g is gravity and U is the mean wind speed.

In Fig. 1 the RCS for the sea, for UHF calculated from (3) for an isotropic spectrum, are shown as a function of the RMS slope, S, for various angles of incidence. The curves for the other frequency bands are similar. In these calculations the Phillips law for the equilibrium range at the spectrum has been used [i.e., $W(K) = 6 \times 10^{-3}\, K^{-4}$], and the limits of integration were taken to be $\pm 4\, S$. The value of the relative dielectric constants used are given in § 3, and for $\theta_i \geq 90°$, the integrand was set at zero. It can be observed that, for the sea, the RCS for vertical polarization is insensitive to the effect of tilts. For all practical purposes, the RCS of the sea (3) for vertical polarization can be taken to be identical to the RCS predicted by the slightly rough scattering theory (2), for no tilts ($\delta = \Psi = 0$). Thus, the RCS of the sea for vertical polarization is approximately given by

$$\sigma_0(\theta)_{VV}^{\mathrm{SEA}} \approx 4\pi\beta^4 \cos^4\theta \left| \frac{(\varepsilon - 1)[\varepsilon(1 + \sin^2\theta) - \sin^2\theta]}{(\varepsilon\cos\theta + \sqrt{\varepsilon - \sin^2\theta})^2} \right|^2 W(2\beta\sin\theta, 0) \qquad (6)$$

$$\text{for} \quad 30° \leq \theta \leq 90° - S.$$

Table I. Sea conditions in the North Atlantic experiment.

Date	Wind speed (m/sec)	Significant wave height (m)	Temperatures (°C) and precipitation
II/6/69	20	Sea 5 Swell 7	Air −3.6 Sea 7.9 Ice crystals
II/10/69	15–17.5	Sea 4 Swell 6	Air 9.0 Sea 8.8 Rain
II/11/69	23–24	Sea 7 Swell 8	Air 5.5 Sea 8.6
II/13/69	17.5–19.5	Sea 7	Air 7.2 Sea 10 Rain showers
II/14/69	18.5–20	Sea 7	Air 6.7 Sea 9.8
II/17/69	2.5	Sea 0.5 Swell 3.5	Air 3.8 Sea 8.5
II/18/69	11–13	Sea 3	Air 8.0 Sea 9.6
II/20/69	14–14.5	Sea 5 Swell 1.2	Air 7.0 Sea 9.8 Rain

Table II. Sea conditions observed in other experiments.

Date	Wind speed (m/sec)	Significant wave height (m)	Observations
XII/9/64	6–7.5	1.8–3	
XII/10/64	2	0.6–1.2	Natural slicks
VII/15/65	5–10	0.9–1.5	Rain
VII/16/65	3.5–6.0	0.6–0.9	
VII/19/65	5.0–7.5	0.9–1.2	
VII/20/65	3.5–6.0	0.6–0.9	
VII/21/65	4–5.5	0.9–1.5	Gusts to 6 m/sec
VII/22/65	5–6	0.9–2.1	1.5–2.4-m swells
VII/23/65	4–6	0.6–1.8	White caps
VII/27/65	0–4	0.15–1.5	Sea squall
VII/28/65	0–2	0.15–0.3	Rain squall
VII/29/65	0.5–7.5	0.3–0.9	White caps

3. *Determination of Ocean-spectra Characteristics from Radar Cross Sections.* Now it is clear that radar cross-section measurements for vertical polarization can be used to obtain ocean wave-height spectra by means of (6); this was shown by Wright (1968).

The RCS data obtained with the 4FR System can be used to investigate the ocean spectrum for wavenumbers of 0.09 cm^{-1} (UHF at 60° depression angle) to 3.51 cm^{-1} (X band at 20° depression angle).[3]

The normalized RCS of the sea is obtained by dividing the RCS of the sea by the illuminated area. The illuminated area is conventionally taken as the surface included within the one-way half-power antenna beamwidth. However, in this study a more precise normalization was used in order to make quantitive comparisons with known oceanographic results. Obviously, the RCS data are obtained with the two-way properties of the antenna, and this is most evident in doppler measurements. Thus, here the illuminated area on the sea is taken as the area included within the two-way half-power antenna beamwidth.

The normalized RCS, in terms of the two-way half-power beamwidth of the antenna, is approximately twice the normalized RCS with the one-way half-power beamwidth, for angles of incidence in which the elevation part of the illuminated area is pulse limited. Furthermore, since the RCS data reported from the NRL-4FR System are median values of an exponentially distributed variable (Rayleigh in amplitude), the data points must be multiplied by 1.441 to convert them to mean values. Hence, the ocean spectra derived from the 4FR data (median values, normalized with the one-way half-power beamwidth) are multiplied by 2.882.

In Tables I and II a summary of the sea conditions during the radar measurements is given.

3. Note that the depression angle is the complement of the angle of incidence, θ, defined earlier (i.e., $90° - \theta$).

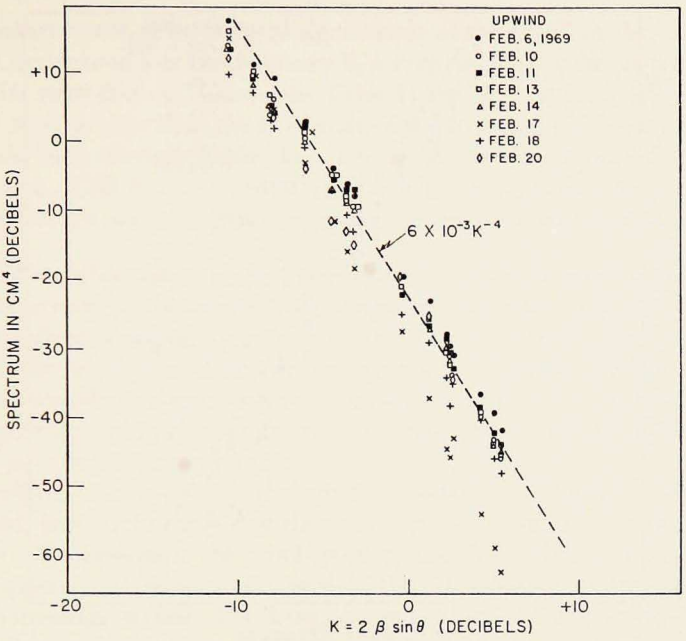

Figure 2. Ocean spectra inferred from vertical RCS data by means of the composite model (upwind). Note the "dip" in the spectrum toward capillary waves on February 17.

The numerical values of the dielectric constants for the sea surface used in this study were obtained from Saxton and Lane (1952): 73–165i for the UHF, 73–85i for the L band, 57.1–36.3i for the C band, and 48.3–34.9i for the X band.

3.1. *The Equilibrium Range of the Ocean Spectrum.* In Figs. 2 and 3 the spectra obtained from the RCS data for vertical polarization for depression angles of 20°, 30°, 45°, and 60° for the North Atlantic measurements are shown; Phillips law is also indicated for comparison.

In Table III the amplitudes and the power law of the spectra were obtained by using a standard least-squares estimation of the slope of the spectra in log-log plot. Surprisingly, the average exponent over the wind direction for the North Atlantic data, excluding February 17 (a calm day), is −3.721, which is in reasonable agreement with Kinsman (1961) (−4.5 law for the frequency spectrum that scales to a −3.75 in wavenumber space).

Kitaigorodskii (1961) postulated a −4-power law for the frequency spectrum (−3.5 law in wavenumber space) for gravity waves of slightly higher frequency than the waves for which Phillips −5-power law applies (−4 law in wavenumber space). Similarly, by dimensional arguments, it is possible to arrive at a general expression for the equilibrium range of the spectrum for gravity waves:

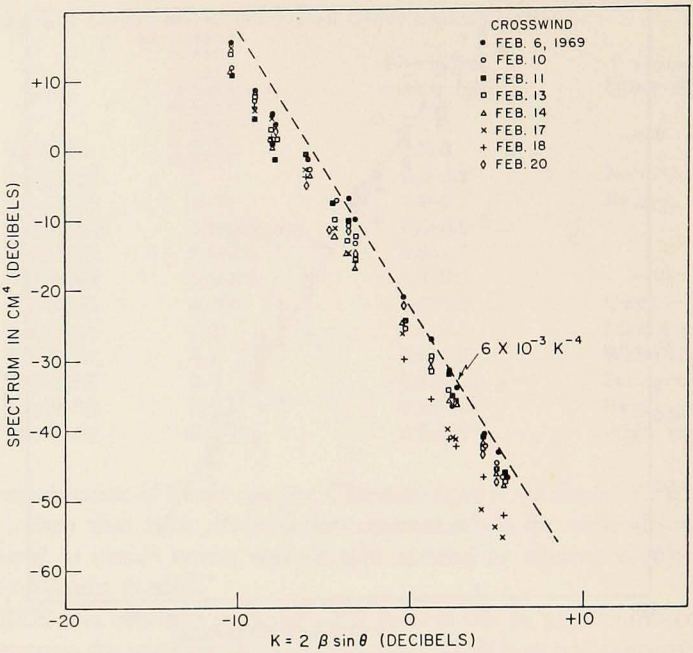

Figure 3. Ocean spectra inferred from vertical RCS data by means of the composite model (crosswind). Note the "dip" in the spectrum toward capillary waves on February 17.

$$W(K) \sim U^{2\nu} g^{-\nu} K^{-(4-\nu)}, \tag{7}$$

where ν is some number.

Some important facts about the spectra obtained from the RCS data via the composite surface-scattering model can be observed. The spectra for February 17, a calm day, have a "dip" toward the capillary region; a similar phenomenon has been reported by Cox (1958) and by Wright and Keller (1971) for wave-

Table III. Amplitude and power law of ocean spectra inferred from the RCS for vertical polarization $W(K) = AK^{-(4-\nu)}$.

Date	Amplitude (A)			Power law $(4-\nu)$		
	Upwind	Downwind	Crosswind	Upwind	Downwind	Crosswind
II/6/69....	9.10 X 10^{-3}	8.58 X 10^{-3}	3.83 X 10^{-3}	3.700	3.774	3.812
II/10/69...	4.32	2.65	2.56	3.775	3.763	3.710
II/11/69...	5.76	4.35	2.71	3.653	3.642	3.584
II/13/69...	5.13	3.66	2.04	3.822	3.695	3.824
II/14/69...	4.55	3.60	1.81	3.664	3.554	3.642
II/18/69...	2.59	2.19	0.92	3.737	3.716	4.206
II/20/69...	4.06	4.18	2.27	3.466	3.626	3.776
Average.....				3.688	3.681	3.793

tank measurements. The physical significance of the "dip" in the spectrum is not well understood yet. On February 6, a very rough day, the air temperature was colder than that on the sea (see Table I) and the amplitude of the spectra is about 70% greater than the amplitude of the spectra for February 11, when the winds were stronger while the air temperature was warmer than the sea temperature. This is a demonstration of the fact that, when the air is colder than the sea, the wave heights are greater for the same wind speed.

3.2. *Wind Dependence of the Ocean Spectrum.* As indicated in (7), the law of the spectrum in the equilibrium range and the wind dependence in this region are directly related for gravity waves. Thus, by means of an independent study of the wind dependence of the spectrum in the equilibrium range, it should be possible to check its power law. Clearly, the wind dependence of the ocean spectrum is identical to the wind dependence of the RCS of the sea for vertical polarization; refer to (6).

Therefore, in this section the wind dependence of the RCS will be investigated, keeping in mind that this is also the wind dependence of the ocean spectrum. To determine the wind speed where the equilibrium or saturation region appears, the wind dependence of the RCS (ocean spectrum) for light winds is investigated first. The Bragg scatterers for the UHF and L-band data are gravity waves and, according to Pierson and Moskowitz (1964), the wind dependence of the frequency spectrum for gravity waves is of the form

$$S(\omega) \sim \exp\left[-0.74(g/\omega U)^4\right], \tag{8}$$

Table IV. Exponential wind dependence of the normalized RCS of the sea, for vertical polarization ($\sigma_0 \sim e^{-C/V}$).

Depr. angle (°)	Norm. RCS $U = \infty$ (db)	C (m/sec)	RMS error (db)	Norm. RCS $U = \infty$ (db)	C (m/sec)	RMS error (db)
	X band (all data)			C band (all data)		
UPWIND						
10.....	−30.471	4.957	3.08	−29.431	4.410	3.36
20.....	−25.890	6.290	3.42	−25.404	5.116	2.38
30.....	−22.079	7.040	2.61	−20.514	7.917	2.31
45.....	−19.724	5.192	2.38	−19.740	4.710	2.25
60.....	−15.453	3.717	2.08	−14.948	3.590	2.50
Average.....		5.439			5.149	
DOWNWIND						
10.....	−30.738	5.285	2.96	−29.709	5.617	2.69
20.....	−26.116	6.773	2.30	−25.126	6.963	1.42
30.....	−23.583	5.970	2.32	−22.298	7.311	2.08
45.....	−19.466	6.474	2.07	−19.149	7.409	2.28
60.....	−15.959	4.069	2.12	−15.925	2.570	2.30
Average.....		5.714			5.974	

Table V. Wind dependence of the normalized RCS of the sea in the saturation region (vertical polarization) ($\sigma_0 \sim U^{2\nu}$).

Depr. angle (°)	Norm. RCS U = 1 m/sec (db)	Exponent (2ν)	RMS error (db)	Norm. RCS U = 1 m/sec (db)	Exponent (2ν)	RMS error (db)
	X band ($U \geq 5$ m/sec)			C band ($U \geq 5$ m/sec)		
UPWIND						
10.....	−35.783	+0.314	2.60	−30.512	+0.040	3.04
20.....	−31.700	+0.353	1.70	−33.374	+0.584	1.60
30.....	−27.856	+0.247	1.51	−29.700	+0.524	2.25
45.....	−27.540	+0.543	1.13	−32.006	+0.964	1.54
60.....	−23.220	+0.540	1.32	−19.851	+0.297	1.81
Average.....		+0.399			+0.482	
	L band ($U \geq 2.5$ m/sec)			UHF ($U \geq 2.5$ m/sec)		
10.....	−33.864	+0.258	3.10	−35.401	+0.074	2.74
20.....	−32.338	+0.567	2.54	−27.235	−0.054	2.04
30.....	−30.468	+0.548	1.94	−29.624	+0.194	1.99
45.....	−25.778	+0.343	2.18	−25.159	+0.048	1.36
60.....	−21.248	+0.388	1.94	−21.232	+0.053	2.56
Average.....		+0.421			+0.063	

where ω is the angular frequency of the gravity waves. By means of the dispersion relationship for gravity waves of infinitesimal amplitude, $\omega^2 = gK$, and the Bragg resonant condition, $K = 2\beta \sin\theta$, it is not difficult to estimate that, for the UHF data, the saturation region should start for wind speeds of 2 to 3 m/sec. For the L band the saturation region should start for wind speeds somewhere between 1 and 2 m/sec.

However, for the C-band and X-band RCS data, the Bragg resonant scatterers are gravity-capillary waves for which the wind dependence is not known. Then, for these wavenumbers the wind dependence will be obtained directly from the RCS data. Various exponential laws of the wind speed were fitted to the C-band and X-band data from all of the experiments (Tables I and II), using the least-squares-fit procedure. An exponential with an inverse linear power of the wind speed yielded the minimum least-squares error in most cases. In a couple of cases, however, an exponential with an inverse square power of the wind was found to give a better fit, but the difference in the goodness of fit was not significant with respect to the exponential with the inverse linear power of the wind speed. Thus, all the C-band and X-band RCS data for vertical polarization were fitted with the exponential law with the inverse linear power of the wind speed.

In Table IV, the parameters obtained in the fitting procedure are given. The average value of the constant in the region of the exponential wind dependence for upwind and downwind data is 5.569 m/sec; this may be related

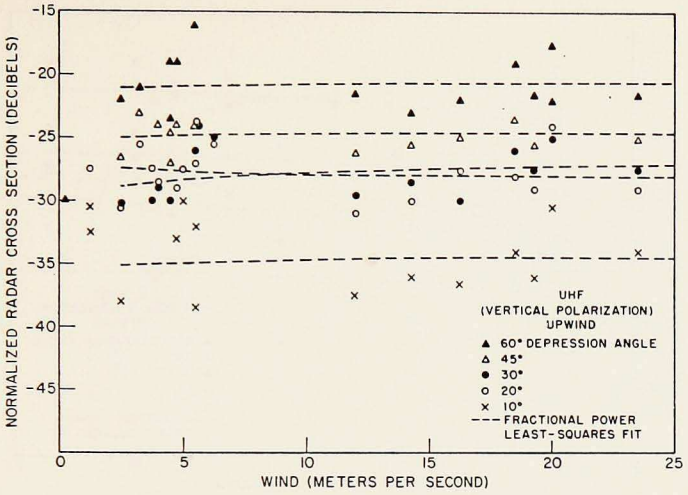

Figure 4. Vertical RCS as a function of wind speed for depression angles of 10°, 20°, 30°, 45°, and 60°, for UHF (upwind).

to the critical wind speed at which instabilities of the water waves occur (i.e., white caps appear on the sea surface for wind speeds of 5 to 7 m/sec). This has been shown by Munk (1947) and Wu (1968, 1969).

Table VI. Wind dependence of the normalized RCS of the sea in the saturation region (vertical polarization) ($\sigma_0 \sim U^{2\nu}$).

Depr. angle (°)	Norm. RCS $U = 1$ m/sec (db)	Exponent (2ν)	RMS error (db)	Norm. RCS $U = 1$ m/sec (db)	Exponent (2ν)	RMS error (db)
	X band ($U \geq 5$ m/sec)			C band ($U \geq 5$ m/sec)		
DOWNWIND						
10.....	−39.874	+0.665	2.79	−40.421	+0.834	1.63
20.....	−32.908	+0.352	1.66	−35.686	+0.698	1.58
30.....	−26.264	+0.000	1.64	−29.684	+0.387	2.17
45.....	−30.303	+0.700	1.04	−32.377	+0.898	1.30
60.....	−24.131	+0.560	2.12	−20.675	+0.281	2.24
Average.....		+0.455			+0.619	
	L band ($U \geq 2.5$ m/sec)			UHF ($U \geq 2.5$ m/sec)		
10.....	−32.784	−0.039	2.98	−33.170	−0.186	3.54
20.....	−30.641	+0.254	2.06	−25.970	−0.235	2.04
30.....	−29.037	+0.304	2.06	−27.877	−0.013	2.32
45.....	−23.669	+0.062	2.36	−23.115	−0.156	2.02
60.....	−19.388	+0.137	2.02	−19.653	−0.124	2.04
Average.....		+0.143			−0.142	

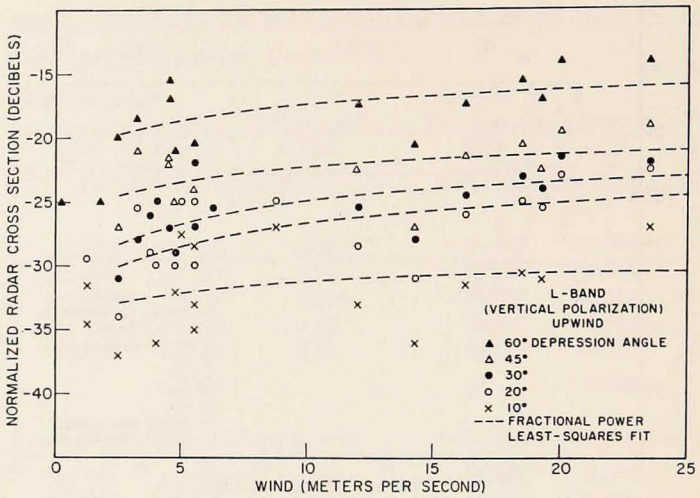

Figure 5. Vertical RCS as a function of wind speed for depression angles of 10°, 20°, 30°, 45°, and 60°, for the L band (upwind).

The RCS data for vertical polarization for large wind speeds were fitted by least-squares with a fractional power law of the wind speed. For the UHF and L band, the saturation region was assumed to start with 2.5 m/sec winds; for the C band and X band, with 5-m/sec winds. In Tables V to VII the solutions for the least-squares fit are given. The average value of the exponent for

Table VII. Wind dependence of the normalized RCS of the sea in the saturation region (vertical polarization) ($\sigma_0 \sim U^{2\nu}$).

Depr. angle (°)	Norm. RCS $U = 1$ m/sec (db)	Exponent (2ν)	RMS error (db)	Norm. RCS $U = 1$ m/sec (db)	Exponent (2ν)	RMS error (db)
	X band ($U \geq 5$ m/sec)			C band ($U \geq 5$ m/sec)		
CROSSWIND						
10.....	−43.120	+0.785	1.41	−40.766	+0.509	2.33
20.....	−39.595	+0.746	1.56	−33.500	+0.209	2.10
45.....	−36.587	+0.977	1.08	−33.058	+0.708	2.07
Average.....		+0.836			+0.475	
	L band ($U \geq 2.5$ m/sec)			UHF ($U \geq 2.5$ m/sec)		
10.....	−33.757	−0.053	2.38	−28.746	−0.572	4.43
20.....	−28.792	−0.030	2.60	−27.256	−0.350	1.68
30.....	−30.705	+0.330	2.13	−26.154	−0.335	1.58
45.....	−25.116	−0.002	2.06	−22.221	−0.355	2.26
60.....	−18.833	−0.046	2.33	−19.388	−0.218	2.03
Average.....		−0.039			−0.366	

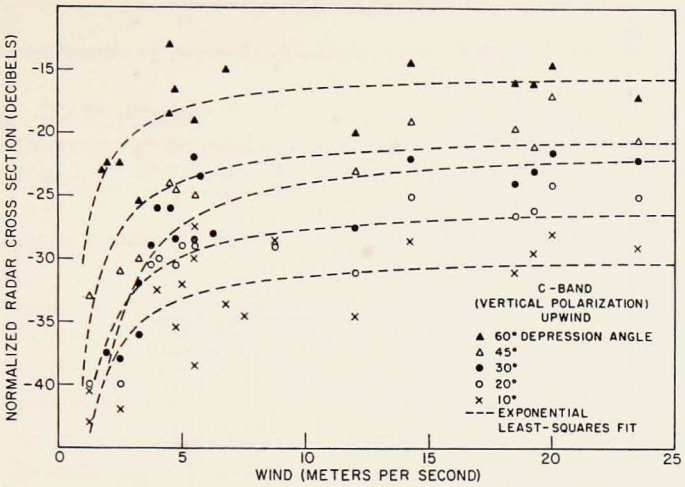

Figure 6. Vertical RCS as a function of wind speed for depression angles of 10°, 20°, 30°, 45°, and 60°, for the C band (upwind).

the C band and X band for upwind, downwind, and crosswind is +0.544; this corresponds to a −3.728 power law for the equilibrium range of the spectrum for these wavenumbers, which is in close agreement with the law obtained earlier.

However, for the L band the average value of the exponent is +0.175, which suggests that, for these wavenumbers, the spectrum should have a −3.922 law; the average exponent for the UHF data is actually negative, −0.148, which would indicate a −4.074 law. Thus, the investigation of the wind dependence of the RCS data for vertical polarization suggests that the power law of the equilibrium range of the ocean spectrum is wavenumber dependent.

In Figs. 4 through 7 the RCS data for upwind (median values and normalized with the one-way half-power beamwidth of the antenna) are shown. In those figures with the UHF and L-band data, the least-square-approximation curves for the fractional wind dependence are shown. In those figures for the C-band and X-band data, the exponential curves obtained by least squares are shown. The fractional wind-dependence curves for $U \geq 5$ m/sec are not very different from those shown for the exponential fit in that region.

4. *Conclusions.* The potential of radar as an oceanographic instrument has been demonstrated in ocean-spectra work. Using RCS data for vertical polarization at 428 MHz, 1228 MHz, 4455 MHz, and 8910 MHz via the composite surface scattering model, it has been possible to investigate the ocean spectrum for wavenumbers of 0.09 cm^{-1} to 3.51 cm^{-1} as a function of wind speed.

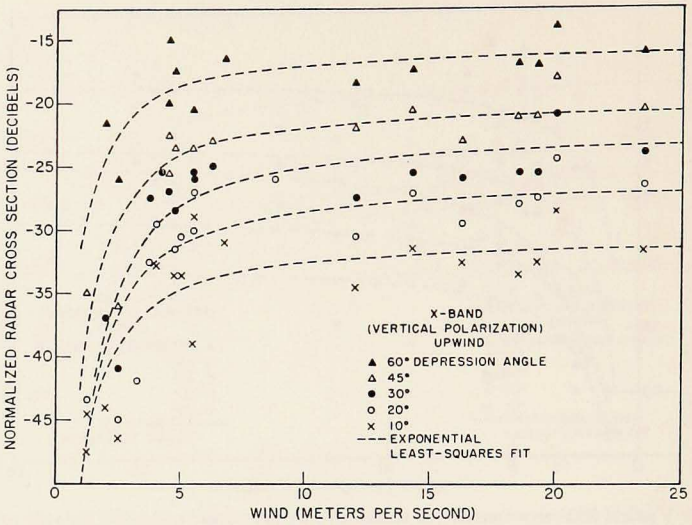

Figure 7. Vertical RCS as a function of wind speed for depression angles of 10°, 20°, 30°, 45°, and 60°, for the X band (upwind).

The following important results have been obtained:

i. The average power law for the equilibrium range of the ocean spectrum for large wavenumbers and wind speeds greater than 5 m/sec is -3.721, which is in close agreement with Kinsman's observations.

ii. The wind dependence of the spectrum for the highest wavenumbers, 1.75 to 3.51 cm^{-1}, in the equilibrium range is of a form that is consistent with the power law of the spectrum.

iii. For light winds, the exponential growth with wind for gravity-capillary waves is of the form $e^{-C/U}$, where $C = 5.569$ m/sec.

iv. A "dip" in the ocean spectrum has been found for water waves of minimum phase velocity for calm seas; previously this phenomenon had been reported for only wave-tank experiments.

Although this investigation has dealt with ocean spectra per se, other oceanographic parameters can be obtained as well. For example, from polarization ratios of the RCS, it is possible to obtain variance in the wave slope; see Wright (1968). From the doppler spectra of a radar sea echo, the waveheight can be determined from the bandwidth, the windspeed from the differential doppler between the maximum of the spectra of horizontal and vertical polarization; see Valenzuela and Laing (1970).

REFERENCES

Cox, C. M.
1958. Measurements of slopes of high-frequency wind waves. J. mar. Res., *16*(3): 199–225.

Cox, C. M., and W. H. Munk
1954. Measurement of the roughness of the sea surface from photographs of the sun's glitter. J. opt. Soc. Am., *44*(11): 838–850.

Crombie D. D.
1955. Doppler spectrum of sea-echo at 13.56 mc/s. Nature, London, *175*: 681–682.

Fuks, I. M.
1966. Contribution to the theory of radio wave scattering on the perturbed sea surface. Izv. Vysh. Uch. Zav., Radiofizika (USSR) *9*(5): 876–887.

Guinard, N. W., and J. C. Daley
1970. An experimental study of a sea-clutter model. IEEE Proc., *58*(4): 543–550.

Guinard, N. W., J. T. Ransone, and J. C. Daley
The variation of the RCS of the sea with increasing roughness. J. geophys. Res. In press.

Kinsman, Blair
1961. Some evidence on the effect of nonlinearity on the position of the equilibrium range in wind-wave spectra. J. geophys. Res., *66*(8): 2411–2415.

Kitaigorodskii, S. A.
1961. Application of the theory of similarity to the analysis of wind generated wave motion as a stochastic process. Izv. Akad. Nauk. SSSR, Ser. Geofiz. *1*: 105–117 (Translation *9*: 73–80).

Munk, W. H.
1947. A critical wind speed for air-sea boundary processes. J. mar. Res., *6*(3): 203–218.

Peake, W. H.
1959. Theory of radar return from terrain. IRE National Convention Record, *7*(1): 27–41.

Phillips, O. M.
1958. The equilibrium range in the spectrum of wind-generated waves. J. fluid Mech., 4(4): 426–434.
1964. A proposed spectral form for fully developed wind seas based on the similarity theory of S. A. Kitaigorodskii. J. geophys. Res., *69*(24): 5181–5190.

Rice, S. O.
1951. Reflection of electromagnetic waves from slightly rough surfaces, Comm. Pure Appl. Math., *4*(2/3): 351–378.

Saxton, J. A., and J. A. Lane
1952. Electrical properties of sea water. Wireless Engng., *29*(10): 269–275.

Semyonov, B. J.
1966. Approximate computation of scattering of electromagnetic waves by rough surface contours. Radio Eng. Electron. Phys., *11*(8): 1179–1187. (Translation).

Strutt, J. W. (Lord Rayleigh)
1894. The theory of sound, *1*, 2nd edition. MacMillan, London. 480 pp.

VALENZUELA, G. R.
1967. Depolarization of e.m. waves by slightly rough surfaces. IEEE Trans., *AP-15*(4): 552–557.

VALENZUELA, G. R.
1968. Scattering of electromagnetic waves from a tilted slightly rough surface. Radio Science, 3(11): 1057–1066.

VALENZUELA, G. R., and M. B. LAING
1970. Study of doppler spectra of radar sea-echo. J. geophys. Res., 75(3): 551–563.

WRIGHT, J. W.
1966. Backscattering from capillary waves with application to seaclutter. IEEE Trans., *AP-14*(6): 749–754.

WRIGHT, J. W.
1968. A new model for sea-clutter. IEEE Trans., *AP-16*(2): 217–223.

WRIGHT, J. W., and W. C. KELLER
Doppler spectra in microwave scattering from wind-waves. Physics of Fluids. In press.

WU, JIN
1968. Laboratory studies of wind-wave interactions, J. fluid Mech., *34*(1): 91–111.
1969. Wind stress and surface roughness at air-sea interface. J. geophys. Res., *74*(2): 444–455.